LNG SUPPRESSION FOAM STABILIZED BY ZIRCONIUM PHOSPHATE NANOPLATELETS

A Thesis

by

LECHENG ZHANG

Submitted to the Office of Graduate and Professional Studies of
Texas A&M University
in partial fulfillment of the requirements for the degree of

MASTER OF SCIENCE

Chair of Committee,	Zhengdong Cheng
Committee Members,	Sam M. Mannan
	Ding Zhu
Head of Department,	M. Nazrul Karim

May 2015

Major Subject: Safety Engineering

ABSTRACT

In this work, a zirconium phosphate based universal foam stabilizer was developed to stabilize and improve performance of firefighting foam and high expansion liquid natural gas (LNG) suppression foam. With the world's increasing demand for natural gas, a large quantity of natural gas is transported in liquid natural gas form. The safety issues related to LNG are of critical concern in LNG process safety. High expansion LNG suppression foam was developed to mitigate accidental LNG spillage. Particle stabilized Pickering emulsion, which mainly the mixture of oil and water, was studied in detail for application in the chemical and oil industries. The advantage of the particle surfactant compared to the conventional surfactant is well understood. A particle stabilized gas-liquid mixture, Pickering foam, is still an emerging topic in soft matter. Pickering foam is studied in this work. Different foam formulas were mixed with propylamine exfoliated ZrP nanoplatelets. Foam stabilities were tested under different conditions, including high salinity and extreme temperatures. We found reduced drainage rate and extra surface stability induced by platelets were two factors which contributed to the excellent stability of our Pickering foam. LN_2 was used to simulate the evaporation process of LNG suppressed by different foam formulas. Experimental results proved LN_2 evaporation rate in the ZrP-PA added foam was modestly lower than conventional foam.

DEDICATION

To my lovely family!

ACKNOWLEDGEMENTS

I would like to appreciate my committee chair, Dr. Zhengdong Cheng and my committee members, Dr. Sam Mannan, Dr. Ding Zhu, for their patient guidance and comprehensive suggestions throughout my research work. I also want to appreciate my friends, colleagues and the department faculties and staffs for making my time at Texas A&M University a great experience. Thanks also go to Xuezhen Wang, Yi-Hsien Yu and Minxiang Zeng for their help during my defense rehearsal.

NOMENCLATURE

AFFF	Aqueous film forming foam
LNG	Liquid natural gas
LN_2	Liquid nitrogen gas
ZrP	Zirconium phosphate
SEM	Scanning electron microscopy
PA	Propyl amine
DI Water	Deionized water
Hi-Ex foam	High expansion foam

TABLE OF CONTENTS

Page

LIST OF FIGURES

Page

LIST OF TABLES

Page

CHAPTER I

INTRODUCTION

Foams and firefighting foams

Conventional foam can be defined as a mixture of gas and liquid, where gas is trapped in the matrix formed by liquid films. From the bubbles on the beer to the foam from shampoos, foam covers every corner in our life. In industry the foams have already been widely utilized in fire-fighting[1], oil recovery[2] and many consumer products[3]. Among them, firefighting foam is an important application for the foam substance. Firefighting foam was invented by Aleksandr Loran in 1902[4] and reformulated in 1960s[5]. The aqueous film forming foam (AFFF) gives fire fighters another powerful tool to extinguish liquid pool fire.

The fire triangle models three necessities for combustion, which are oxygen, fuel and ignition source [Figure 1]. The firefighting foam extinguishes fires by suffocating them, that means remove the oxygen from combustion process. After the foam solution being injected into the generator, the foam can expand as much as thousand times within several seconds. Firefighting foam, as a significant innovation in fire protection, greatly facilitates extinguishments of liquid pool fire.[6, 7]

Figure 1. Fire triangle

Generally, firefighting foam can be classified into two categories: Class A foam and Class B foam. Obviously, Class A foam is used to fight a type A fire, which is ordinary solid combustible and Class B foam can be applied on flammable liquid and gas, which is the type B fire.[8]

Foam can be stabilized either by surfactant or by solid particles.[9] The conventional foams are usually stabilized by surfactant and particles stabilized foam will be discussed in later section soon. Including organic amphiphilic molecules and some proteins, different chemicals can be used as surfactants to stabilize foams. The function of surfactant in foam system is complex and not very clear .[9] Surfactant helps stabilizing foam bubbles in many ways. From the view of thermodynamics, the main effect of surfactant is reducing the surface tension between gas and liquid phase. It is well known that some surfactant can reduce interfacial tension but cannot stabilize foam effectively. To describe stabilization process better, we have to understand how the surfactant functionalizes. To elaborate this problem further on the other aspect, we should take a look at Figure 2 first.[10] Figure 2 presents the relationship between surface tension of the

gas/liquid interface and concentration of the surfactant. When concentrations of surfactants are below critical micelle concentration (CMC), interfacial tension decreases with concentration of surfactant increasing. After CMC, surfactant are saturated on the interface and the newly adding surfactant no long goes to the interface, instead, aggregates to form micelles to be suspended in the bulk solution.

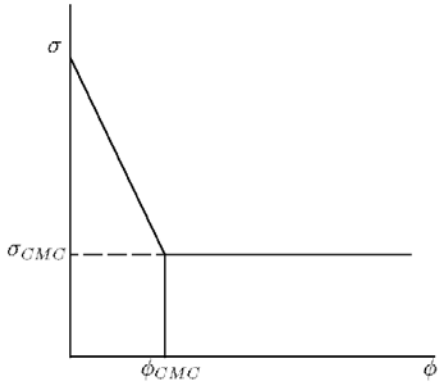

Figure 2. Surface tension σ versus surfactant concentration ϕ[10]

The relationship in Figure 2 can be approximately represented as:

$$\frac{d\sigma}{d\phi} = \frac{\sigma - \sigma_{cmc}}{\phi_{cmc}} \qquad 1\text{-}1$$

This formula shows how fast a surfactant can reach its CMC with surfactant concentration change.

On the other hand, rupturing of a bubble is because the concentration of surfactant on a thin film is too low to maintain the low interfacial tension. The Gibbs elasticity (E_g) is another thermodynamics term to present elastic property of a foam film.[11] According to the definition,

$$E_g = A \times \frac{\mathrm{d}\sigma}{\mathrm{dA}} \qquad 1\text{-}2$$

However there is no direct correlation between interfacial tension (σ) and area (A). So we have to rearrange formula (1-2) to,

$$E_g = A \times \frac{\mathrm{d}\sigma}{\mathrm{d}\phi} \times \frac{d\phi}{dA} \qquad 1\text{-}3$$

We have mentioned $\frac{\mathrm{d}\sigma}{\mathrm{d}\phi}$ term before, which is the interfacial tension changing rate with the surfactant concentration. We get another interesting term in formula 1-3. The $\frac{d\phi}{dA}$ term tells us elasticity of foam thin film is also related with the surfactant concentration change with surface area. If explained in this way, the $\frac{d\phi}{dA}$ term is still enigmatic. We always can get a relationship between surface area (A) and surfactant moles on the surface (N_s),

$$\frac{\mathrm{dA}}{\mathrm{A}} = \frac{d\mathrm{Ns}}{\mathrm{Ns}} \qquad 1\text{-}4$$

So, 1-3 can be rearranged to,

$$E_g = \mathrm{Ns} \times \frac{\mathrm{d}\sigma}{\mathrm{d}\phi} \times \frac{d\phi}{d\mathrm{Ns}} \qquad 1\text{-}5$$

Now this formula is more explicit. From formula 1-5, we know elasticity of a foam thin film is related with the rate to reach CMC, the rate of surfactant to absorb on the film and the concentration of surfactant on the film.[10]

Formula 1-5 tells us what a role surfactant plays in stabilizing foam bubble thermodynamically. However, foam is a metastable system. Drainage and coarsening process will also unstabilize foam. Drainage describes the redistribution of solvent phase in foam and coarsening describes redistribution of gas in foam.

Pickering foams and their advantage

Previous section we were focusing on surfactant stabilized foam. Different from conventional foams, Pickering foams are stabilized with solid particles.[9, 12] Different efforts had been made to stabilize foam with different particles.[13, 14] The energy required to remove the particle from the interface is given by,

$$E = \pi r^2 \gamma_{interface}(1 \pm \cos\theta)^2 \qquad 1\text{-}6$$

r is the diameter of platelet

$\gamma_{interface}$ is the interfacial tension between air and gas

Θ is the contact angle of liquid phase

According to this formula if particles exhibit contact a 90° angle and interfacial tension is 50 mN/m, then the energy needed to remove particle on interface would depend on radius of particle only. The relationship is shown as Figure 3. The required energy is higher, as particle is larger.

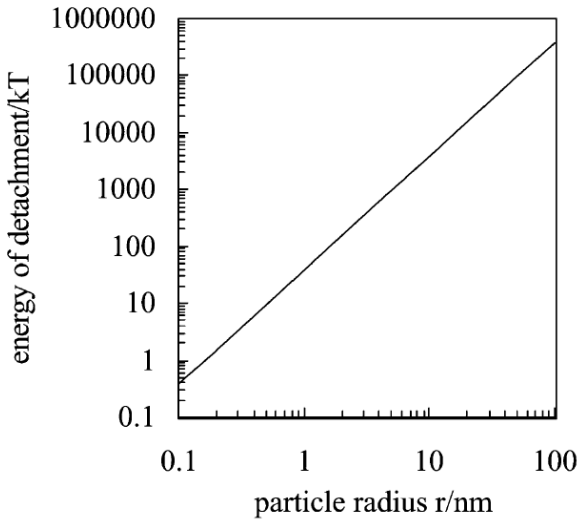

Figure 3. Dependence of energy to remove particle on interface with particle radius[12]

Another factor should be taken into account is the capillary pressure. The capillary pressure produced by the gap between particles can be presented as formula 1-7. With high capillary pressure, phases on both sides of particles can be prevented to merge together (Shown as Figure 4).

$$P_C^{max} \sim 2 \times \frac{\gamma_{ow}}{h} \qquad 1\text{-}7$$

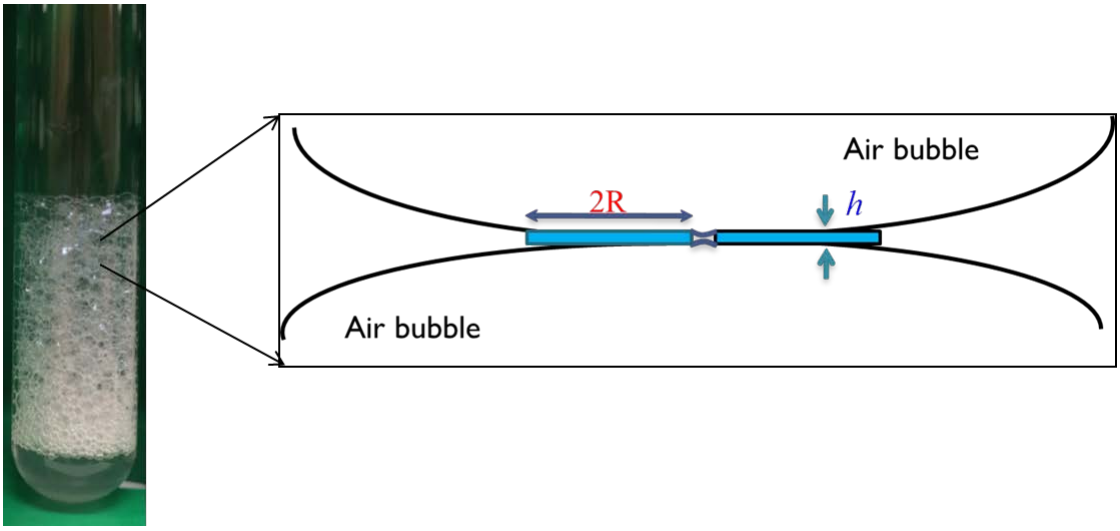

Figure 4. Scheme for capillary pressure between particle gap

Therefore, we count on (1-6) and (1-7) together: larger diameter and thinner thickness would be preferred to use particles to stabilize two phases. If we place the diameter, 2R and thickness h together in aspect ratio expression, $\xi = 2R/h$, then we get the message that large aspect ratio is desired for particles to stabilize interfaces.

LNG and LNG hazards

Natural gas is one of the major power sources of the world. In 2012, the world natural gas consumption amount is 119,568 Billion Cubic Feet (BCF).[15] With this large consumption amount, the LNG trading amount is tremendous. 36,751 BCF natural gas were exported during 2012.[15] Most of these trading amounts were transported in liquid form of natural gas, which is known by LNG. Natural gas would be cooled down below -162 C° to be liquefied, transported and stored with special cryogenic equipments. After arriving in destination, LNG will be regasified in terminal and delivered to consumer through pipelines. The LNG transportation loop involves thousands of sophistically

designed components, which fulfils two tasks, keeping LNG cool and sustaining the pressure caused by gasification.

However, catastrophe happens when any of these components fails. Spilled LNG will quickly evaporated and form a combustible vapor cloud.[16, 17] The leakage of LNG can cause property losses and casualties if not handled properly. On 20th October 1944, Cleveland Ohio, a crack on a LNG tank initiated a Domino Effect and claimed 128 life.[18] The later investigation showed the inner tanks was made by nickle steel, which is susceptible to cracking under low temperature. Also, bad facility siting and absence of diking contributed to this tragedy. The LNG facilities within U.S. have been proper functioning without major accidents for decades since the Cleveland accident. Nevertheless, an accident occurred in Skikda, Algeria, alerted the industry again how ugly an LNG spill accident could be. On January 19, 2004, a boiler in the Skikda LNG facility exploded and triggered a series of cascading vapor cloud explosions. It caused 27 deaths, 72 injuries and destroyed two thirds of the facility. The root cause of this incident is lacking of automatic shut-down system.[19]

The hazards with LNG are not limited to combustion of the vapor cloud. Also, due to its ultra-low boiling temperature, vaporization caused physical expansion has also been noted as a potential hazard for LNG.

Fortunately, by learning from mistakes, we understand more and more about LNG property and LNG hazards. People learnt from these accidents, developed reliable system such as, back up cryogenic system, mitigation methods like suppression foam

and remediation method like diking and slump, trying to utilize LNG safely and effectively.

High-expansion foam: mitigation for LNG

High-expansion foam has been recognized as a mitigation method for LNG spill since the 1970's.[20] Different from the common aqueous firefighting foam, which suffocates fire from oxygen, the LNG high expansion foam applies a blanket on the low temperature liquefied hydrocarbon to isolate LNG from atmosphere, hence, decreases the evaporation rate. Meanwhile, the thick foam blanket could heat up the evaporated LNG (Shown as Figure 5). As a result, escaped natural gas has lower density when the temperature is higher. Low density can endow the evaporated natural gas higher buoyancy, so evaporated LNG can rise higher. It is well known that the ignition sources mainly exist near ground altitude. If the evaporated LNG can rise higher, even the concentration is within the explosion limit, the natural gas won't be ignited without an ignition source.

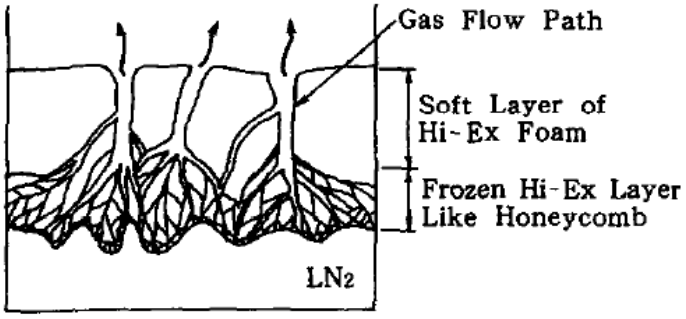

Figure 5. Scheme of high expansion foam applied on LN_2[20]

Research objectives

Objective 1: Observe effectiveness of ZrP foam stabilizer by foam volume measurement.

Objective 2: Investigate the mechanism for ZrP Nanoplate stabilizing Hi-Ex Foam by drainage rate test.

Objective 3: Test foam stability under harsh condition, including low temperature and high salinity.

Objective 4: Use Liquid nitrogen gas (LN_2) to simulate the vaporization of LNG. Measure and compare result with and without ZrP foam stabilizer.

CHAPTER II

LITERATURE REVIEW

Foam rheology and morphology have attracted a lot of research interests. Its application is not only limited in firefighting, but it also has many applications in other industry fields, such as heat insulation and noise insulation. Juan S. Guevara, a previous student in our group, had investigated Pickering foams generated by ZrP nano plates.[21] In his work, he had a comprehensive investigation on Pickering foams generated by different aspect ratios of ZrP with different weight percentage of particles, and proposed the mechanism of foam bubble collapsing. From literature reviewing, we found that natural clay platelets have been used as foam stabilization also, such as Laponite and layered double hydroxides modified with surfactant have served as foam stabilizers.[22, 23] Mechanisms have been proposed by previous research to explain why solid particles can stabilize aqueous foams. The nano-scale hydrophilic platelets can aggregate at on the plateau borders between bubbles[24] and irreversibly adsorb onto the liquid/air interface.[12] Also, some other factors will affect particle's function as a interfacial stabilizers, including hydrophobicity[12, 25-27], size[28, 29],shape[22, 30], aspect ratio[31], and concentration[27, 32-34]. Contradictory results has been reported about the optimal particle size and hydrophobicity of nano particles for foam stabilization.[35] Tang et al.[24] applied silica spheres together with surfactants to stabilize foams. In their paper, they stated stability of foam could be enhanced using smaller particles. Whereas, Hudales et al.[36] stated a better foam stability can be achieved by larger-size hydrophilic quartz particles. From literature reviewing, we found a lot previous works have been done by our group and other groups

on particles stabilized foam, and it is promising to stabilize different foams, such as high expansion foam or aqueous firefighting foam with our nanoplatelets foam stabilizer.

ZrP crystal and ZrP nano sheets

α-Zirconium phosphate (α-ZrP, $Zr(HPO_4)_2 \cdot H_2O$) is a monoclinic crystal with P_{21}/C space group. Cell dimension is a=9.076 ± 0.003 Å, b=5.298 ± 0.006 Å, c=16.22 ± 0.02 Å, β=111.5± 0.1°. Zirconium atoms form a plane and each zirconium atom sits in the center of an octahedron center. The crystal plane is duplicated and forms a layered structure as Figure 6 shows.[37] Different method has been reported to synthesize α-ZrP. As early as 1964, Clearfield et al., used zirconyl chloride to recrystallize in phosphoric acid and collected the precipitate.[38] However, crystal growth is slow by this method. The current hydrothermal method we are using nowadays was not formally published until 1991.[39]

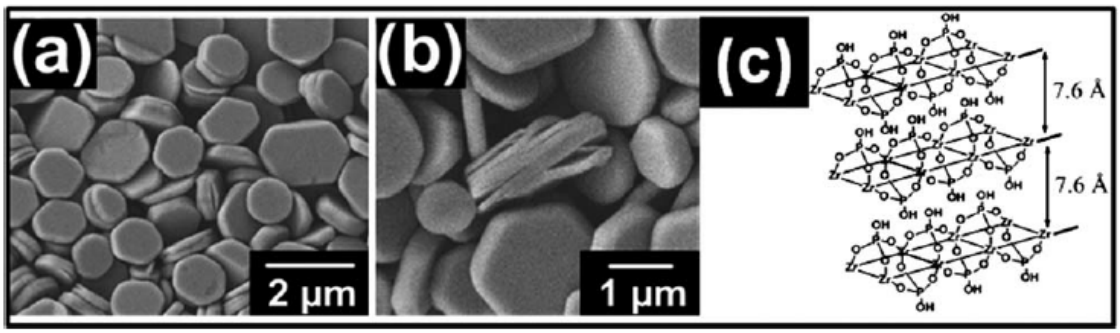

Figure 6. SEM pictures of ZrP and α-ZrP crystal structure[40]

At the meantime, there are lots of literatures worked on the exfoliation of ZrP. Different guest molecules were used to intercalated with ZrP by ion-exchange.[41-45]

Among them the intercalation of ZrP with n-propylamine through ion-exchange effect had been studied comprehensively.[46-48] Mejia et al. reported preparing Pickering emulsions with surface functionalized ZrP nano-platelets.[40]

Pickering foam and Pickering emulsion stabilized by ZrP platelets

Exfoliated ZrP nano-platelets exhibited great potential to be functionalized as new generation surfactants. In 2012, Mejia et al. proposed a general method to exfoliate ZrP layered structures and produce ZrP mono layer Janus particles.[40] Octadecyl isocyanate was employed to modify ZrP crystal surface first. Isocyanate can graft with the hydroxyl group on pristine crystal surface and anchored on the crystal. Then tetrabutyl amino hydroxide was applied to exfoliate the surface modified ZrP crystal to generate single layered Janus and Gemini particles. (Figure 7)

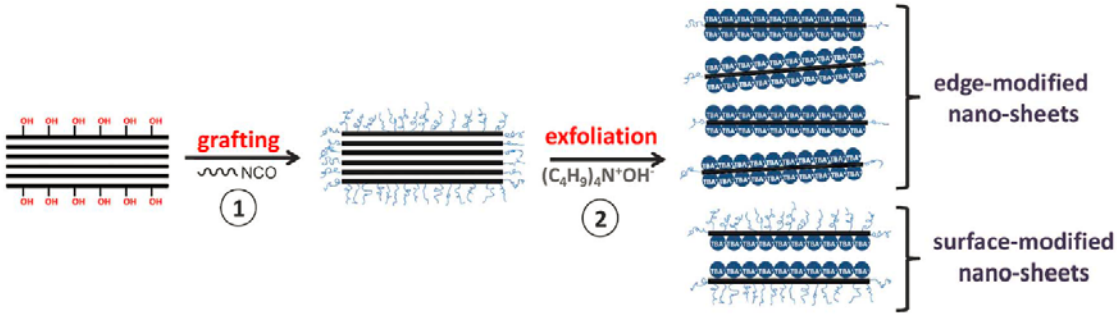

Figure 7. Scheme of ZrP surface modification with isocyanate and crystal exfoliation to generate surface active nanoplatelets[40]

The as-synthesized nanoplatelets are proved to be surface active. Large aspect ratio (~320)[40] endows the nanoplatelets strong absorption energy onto the oil/water interface (according to equation 1-6). Also, the surface amphiphilic modification further decreases

interfacial tension. These surface active Janus platelets had been used to stabilize oil/water interface by mixing oil and water phases to generate microemulsions (shown as Figure 8).[40]

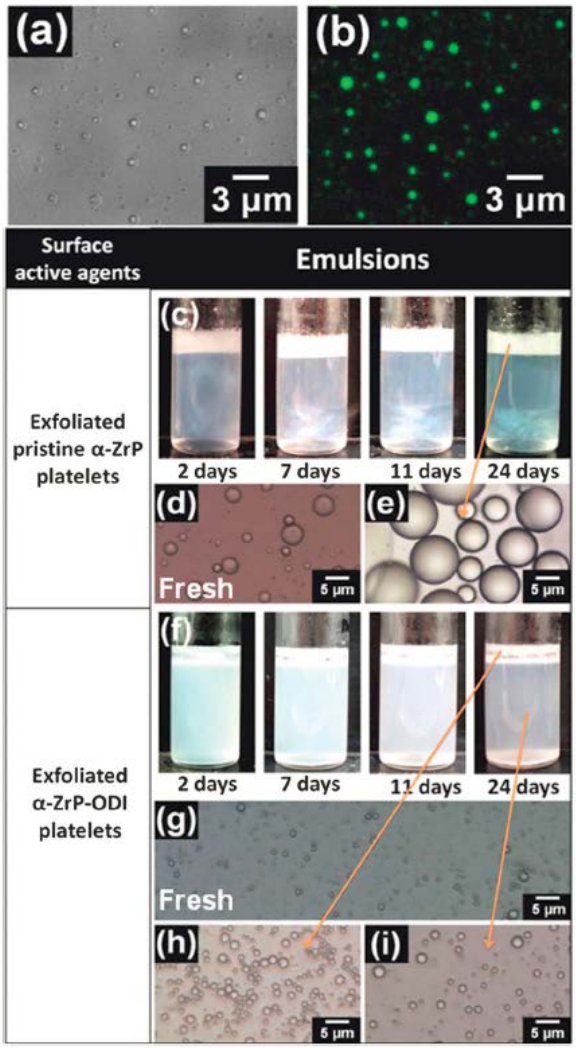

Figure 8. a) Optical image of emulsions generated by surface active ZrP. b) Con-focal image of emulsions generated by surface active ZrP. c) Photos of emulsions generated with surface non-active ZrP changing with time. d) Optical image of emulsions generated by surface non-active ZrP. e) Optical image of emulsions generated by surface non-active ZrP after 24 days. f) Photos of emulsions generated with surface active ZrP changing with time. g) Optical image of emulsions generated by surface non-active ZrP. h), i) Optical image of emulsions generated by surface non-active ZrP after 24 days.[40]

Guevara et al. used propyl amine exfoliate ZrP to generate Pickering foam system.[21] They found the high aspect ratio platelets help stabilize foam up to several weeks. The performance was related with the platelet size and surface hydrophobicity. Interestingly, in their paper, they stated hydrophobicity and particle size was conflicted with each other. Though high hydrophobicity can stabilize foam, it also can repel platelets and cause platelets aggregation. So they conclude that using low aspect ratio particle with high hydrophobicity or large aspect ratio particle with mediate hydrophobicity would be a good formula for foam stabilization. Also they observed that by changing the propyl amine/ZrP ratio, hydrophobicity of the system would be changed also. Their assumption is because more propyl amine can make ZrP platelets surface hydrophobic. However, it also could be the excessive propyl amine diffused into system causing the rise of hydrophobicity. With scanning electron microscopy (SEM) they studied foam structure in detail. SEM pictures (Figure 9) revealed several layers of ZrP stacked together on the borders between bubbles. They propose the jammed boundaries actually were hindering the draining process in foam boundaries.

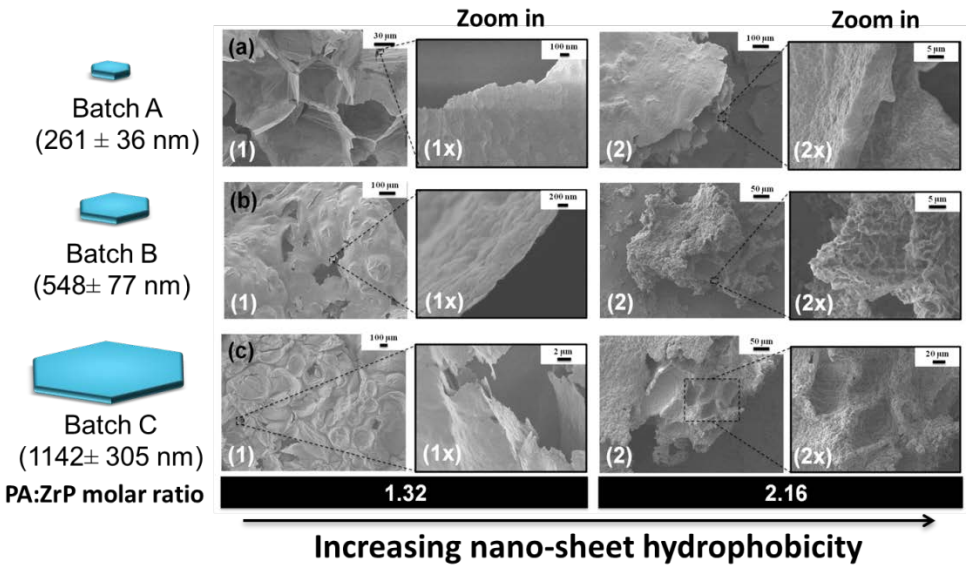

Figure 9. SEM pictures revealing the ZrP-PA Pickering foam border

Blanketing effect of expansion foam on LNG

With the quick booming in LNG industry, the research in LNG is kind of behind. For the LNG high expansion foam, the most impacted work would be Takeno's paper publish in 1996.[20] Takeno used LN_2 as model to simulate LNG's behaviors. The simulation illustrated foam evolution after covering the cryogenic liquid and they also measured the temperature profile at different foam depth. It is worthy to mention that LN_2 simulated situations won't be exactly same with LNG spillage by taking intrinsic differences between two different gas species, such as boiling point difference, heat capacity and heavier molecular, into consideration. LN_2 has higher heat capacity and heavier molecular weight than LNG, which causes LN_2 simulation would be the "worst scenario" of LNG spillage. In Takeno's paper liquid evaporation speed, temperature rise effect had been evaluated also.

Recently, Bin Zhang et al. from Mary Kay O'Connor Process Safety Center published a paper on blanket effect of high expansion foam on LNG.[49] He designed a sophisticated setup to monitor the vaporization process of LNG. The setup was composited by a balance in the bottom to measure the mass change, polystyrene container to isolate LN_2, fence for high expansion foam and several accessories for temperature measurement (Figure 10). He observed that heat conduction through the container cannot be reduced by the high expansion foam blanket. However, the blanket helps reduced up to 70% of heat input from convection and ambient thermal radiation. In his paper, Bin also mentioned the drainage rate is the essential factor determines vaporization rate of foam-covered LNG. He proposed drainage rate was affected by external conditions, such as radiation, and internal properties of foam, such as foam stability.

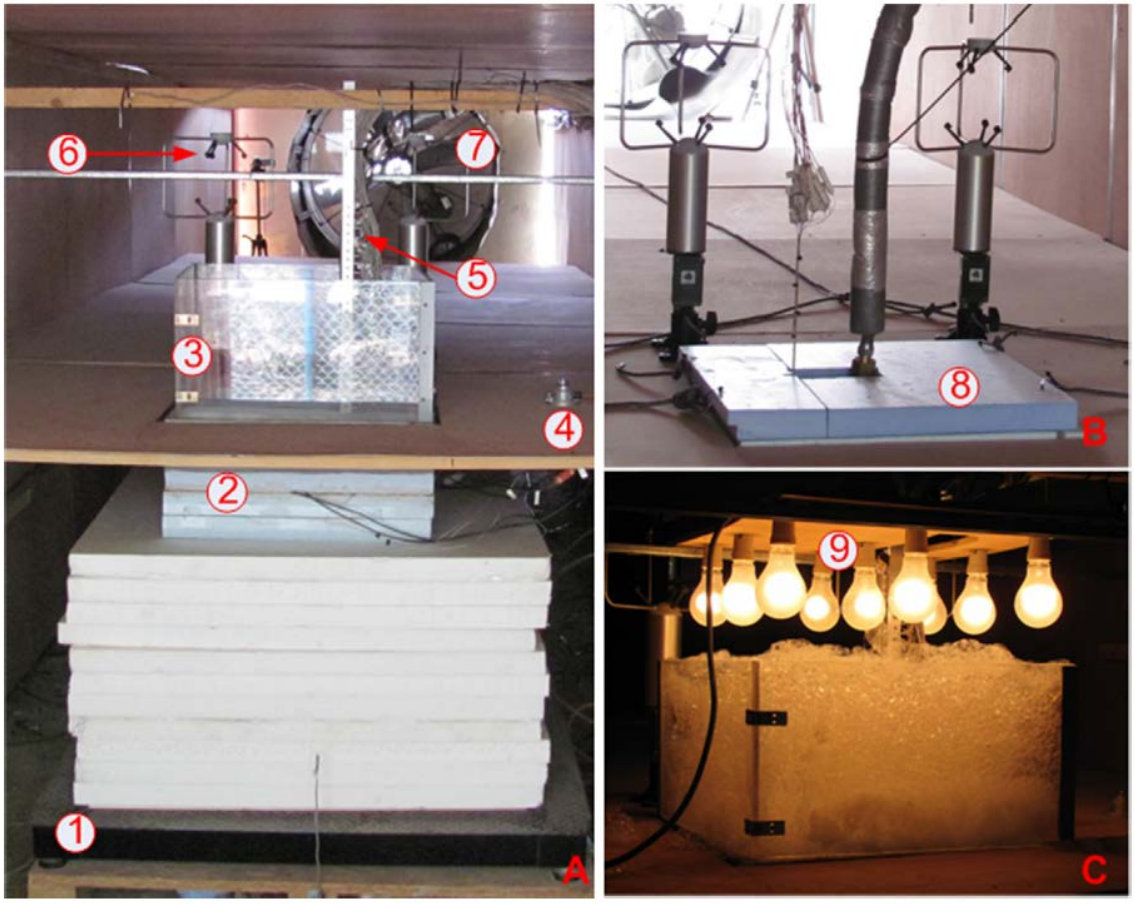

Figure 10. A. Setup for convection test. B. Setup for conduction test. C. Polystyrene container for LN_2. D. Bulbs panel for radiation test. (A is the setup to measure the convection and radiation interference, B is the setup to measure thermal conduction interference, C the lamp panel for thermal radiation test. 1 balance; 2 polystyrene container;3 fence for foam containment; 4 radiation sensor; 5 thermocouples; 6 anemometer; 7 fan; 8 polystyrene lid; 9 lamp panel) [49]

Foam drainage and ripening

Foam had been applied into different fields, such as mineral extraction, cushion buffer or food industry, where the stability of foam is critical for these applications. Most of time stable foam which can last longer time would be desired in application. Foam decaying process can be described into two stages, which are foam drainage and foam ripening[9, 50].

Foam drainage describe phenomenon that the liquid phase within foam flow out through the aqueous boundary between foam bubbles. This may lead into instability of foam respect to film rupture which is not desired. The foam drainage phenomenon is similar with the flow in solid porous structures. Whereas, tit can be describe with Dacey's law. A generalized expression describing foam drainage phenomenon will be:

$$\mu\frac{\partial\epsilon}{\partial t}+\rho g\cdot\nabla(k(\epsilon)\epsilon)-\frac{\gamma\delta_{\epsilon}^{\frac{1}{2}}}{L}\nabla\left(k(\epsilon)\nabla\epsilon^{\frac{1}{2}}\right)=0 \qquad 2\text{-}1$$

Where ϵ is the liquid content, $k(\epsilon)$ is the permeability, μ is the viscosity.[51] The other factor change foam stability is the foam ripening phenomenon which is a redistribution of gas within foam bubbles. The diffusion of gas between adjacent bubbles will drive into a growth in average foam bubble size and finally bubble disappearing. [9]

CHAPTER III

ZRP SYNTHESIS AND EXFOLIATION

According to the foam expansion ratio, firefighting foam can be classified into two sorts: low-expansion foam and high-expansion foam. Because of its good wetting properties, low expansion foams have been proved to be more effective in extinguishing forest fires than high expansion foams by directly spraying onto fire. On the other hand, high expansion foams are normally used as LNG suppression foam, as it is more viscous and tend to adhere to vertical surfaces.[8] There are thousands of different firefighting foam formulas in the market. Ingredients in these formulas vary from one another. A conventional stabilizer, mainly amphiphilic polymer, can't be compatible with all these ingredients. Thus, another drawback for the conventional firefighting foam stabilizer is its limitation on application. A universal foam stabilizer will be desired to stabilize foams with different expansion ratios. Different from the conventional stabilizer, our ZrP plates stabilize foam bubbles by reducing foam drainage rate and preventing foam bubble collapsing. These fundamental changes on the foam property may potentially lead to universal application on different formulas. In this chapter, the detail of chemical synthesis will be recorded, thoughts in experiment design will be elaborated and observations on the experiment will be illustrated.

Synthesis of ZrP nano particles

Different sizes of ZrP pristine crystals are synthesized with different hydrothermal methods, as described in Shuai[52] and Sun's paper[53]. Particles with 200nm and 1000nm mean size are synthesized with the reflux method and hydrothermal method, respectively.

In a typical 200nm reflux batch, 6g Zirconyl chloride is mixed with 12 M phosphoric acid and then heated at 95 ℃ for 24 hours. After harvesting, products will be washed for three times with deionized water (DI Water) and dried in oven. Freeze drying had also been tried once. Later experiment didn't show obvious difference between freeze-dried ZrP crystal and oven-dried crystal. The synthesized material will be stored properly in centrifuge tube for later use.

Particles with 1000 nm mean size are synthesized with autoclaves. In a typical batch, 2g Zirconyl chloride, mixed with 12 M phosphoric acid, will be added in to a Teflon lining and stirred for 30 minutes to 1 hour. After mixing, the autoclave will be put in 200℃ oven for 24 hours. Products will be washed three times with DI water and dried in oven after harvesting. The synthesized material will be stored properly in centrifuge tube for later using.

Exfoliation and modification of ZrP with propylamine

The ZrP pristine powder synthesized in the previous section was first suspended in DI water for days, to have the crystal saturated with water. This step can facilitate the exfoliation of ZrP particles and increase the possibility for a successful exfoliation. The normal protocol for the experiment will be 0.5 g ZrP disolved in specific amount of DI water to make sure final weight concentration would be satisfied. The amount of propylamine used in exfoliation will be calculated with 1:1 molar ratio.[54] However, since we changed the weight percentage of ZrP for different ZrP concentrations, we were using different liquid volumn for each part in different systems. Each propylamine exfoliated system will be described in detail in Table 1. In a standdard protocol, 0.5

mol/L propylamine will be injected into the system with an injection pump at a speed between 2 to 4 ml/hour while keeping stirring with magnetic bar. After amine injection, the system will be kept stirring for better intercalation under room temperature for up to 7 days to let the exfoliation fully processed.

Table 1 Ingredients for different concentration of ZrP

	4% ZrP	3% ZrP	2% ZrP
ZrP Powder	0.8 g	0.6 g	0.4 g
DI Water	15.14 ml	16.35 ml	17.57 ml
0.5 M Propylamine	4.86 ml	3.65 ml	2.43 ml

Transmitance electronic microscope (TEM) are applied to characterize the material before and after ZrP Exfoliation. Figure 11 shows a collection of TEM image of different ZrP crystals in different exfoliation stages. Picture A and Picture B show the unexfoliated ZrP inorganic crystal morphology. The unexfoliated ZrP has heavey contrast under TEM, which means the material is thick, so there wouldn't be so much transmitted electrons. In pictures C and D, I observed two different partially exfoliated ZrP plate. These nano scale pictures are indirect evidences for the exfoliation process. As in previous paper mentioned,[52] the propylamine intercalted into the inter atomic layer of the ZrP crystal. Through ion-exchange reaction the hydrogen bond connecting the layers is weaken and separate fall apart. Picture E in Figure 11 shows the exfoliated thin layer of ZrP crystal.

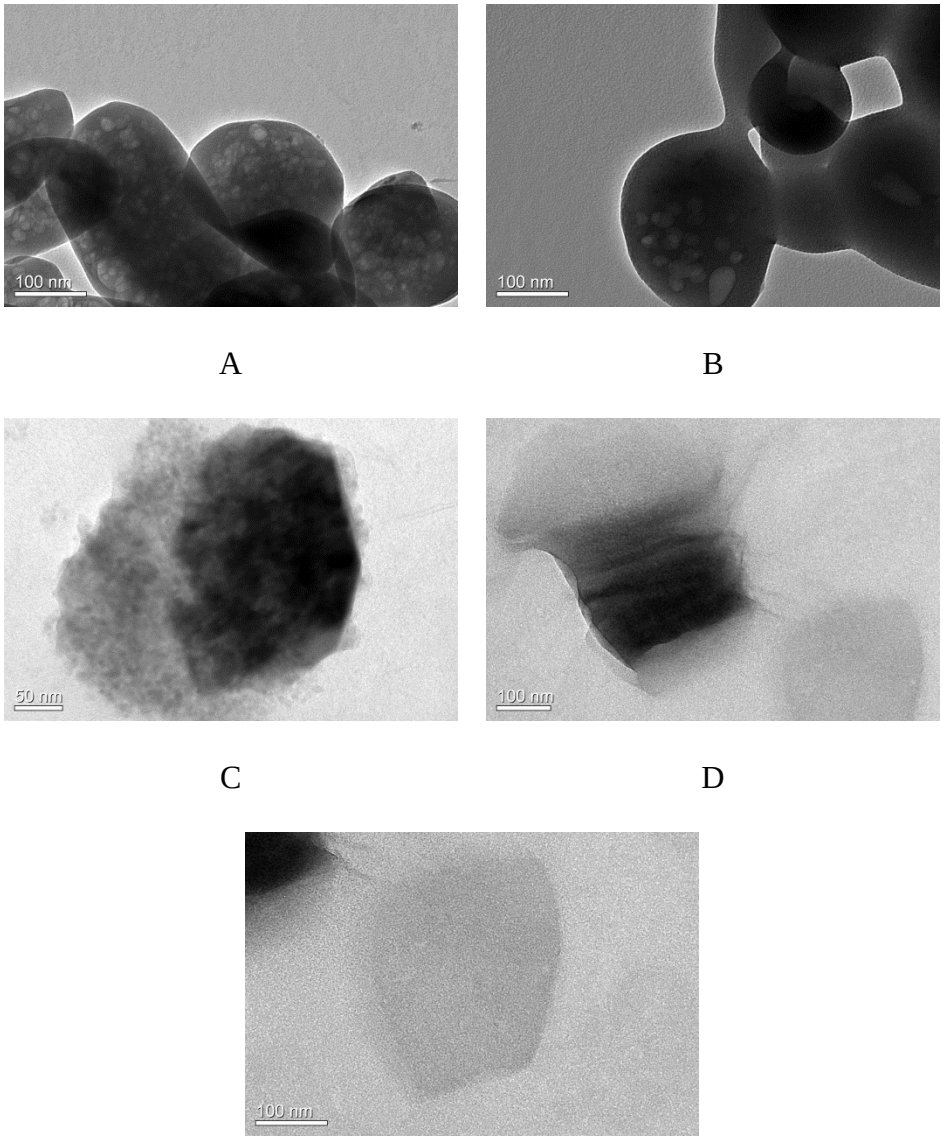

Figure 11. TEM image of ZrP: A, B. Unexfoliated ZrP Crystal. C,D. Partially exfoliated ZrP platelets. E. totally exfoliated ZrP platelet (also shown in right bottom part of picture D).

CHAPTER IV

FOAM STABILITY AND LN_2 EVAPORATION TEST

Foam volume decaying test and bubble morphology with different formulas

APG based aqueous firefighting foam formula

To obtain aqueous foams with different firefighting foam formula stabilized by ZrP–PA nano-sheets, all final concentrations of foam formula and ZrP particles of the final system will be calculated ahead. Normally, 1 ml of foam formula with calculated concentration will be mixed with 1ml ZrP–PA nano-sheets with proper concentration in a glass test tube. Each suspension is vigorously shaken by hand for a period of 30 s to generate enough foam. To test the performance of the ZrP foam stabilizer, we want to screen it with different type of the foaming systems. In our experiment we used three different foam formulas: a non-ionic surfactant APG based AFFF firefighting foam adopted from US PATENT 520793250[55] an ionic surfactant SDS based high expansion firefighting foam adopted from US PATENT 444201851[56] and a high expansion firefighting foam in market with commercial name 'Fireguard C2' foam.

Firstly, a firefighting foam formula was adopted from the book 'Foam engineering' and modified by adding ZrP foam stabilizer[9] (the original formula is from US patent 5,207,932).[55] The formula is composited by Alkyl Poly Glucose (APG, From Dow Corning Company), Butyl Ether and Ethylene Glycol (EG). The detail formula is listed in Table 2. In this test, 4 samples are prepared, including a 2 ml foam concentrate, a 1 ml foam concentrate with 1 ml DI water, a 1 ml foam concentrate with 1 ml 4% 1000nm ZrP-PA, a 1 ml foam concentrate with 1 ml 4% 200nm ZrP-PA.

Table 2 Foam formula based on APG

Foam concentrate formula based on APG	
APG	85%
Butyl Ether	10%
EG	5%

Every half an hour the image of the system was taken for later foam height measurement. A ruler was put beside test tube as a reference to measure the foam height. And each time the camera should maintain the same height relatively to system to take the picture. Pictures right after mixing and 16 hours later are shown as Figure 12. After all pictures taken at different time, the foam heights were measured and shown in Figure 13. The data show the foam with ZrP-PA stabilizer have a better stability compared to the ones without ZrP-PA added in. The data from the APG foam showed a promising result.

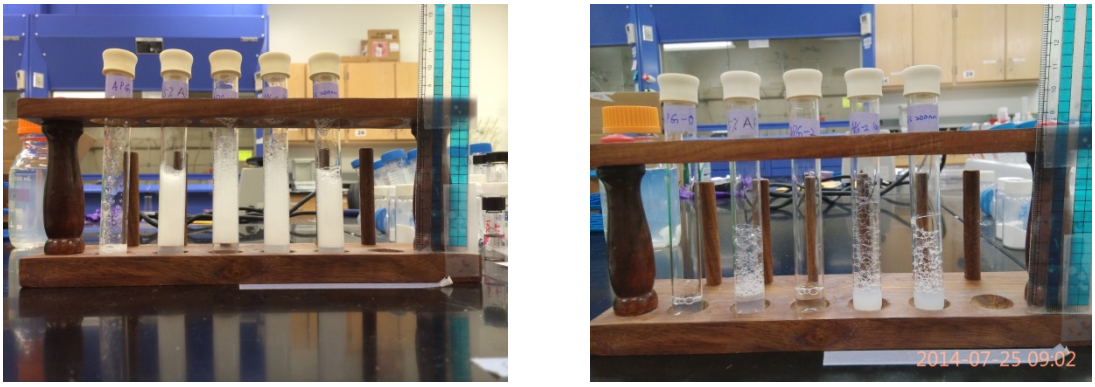

Figure 12. Picture of the foam test right after mixing (left) and 16 hours later (right). Annotation: APG-2 stands for the APG based formula

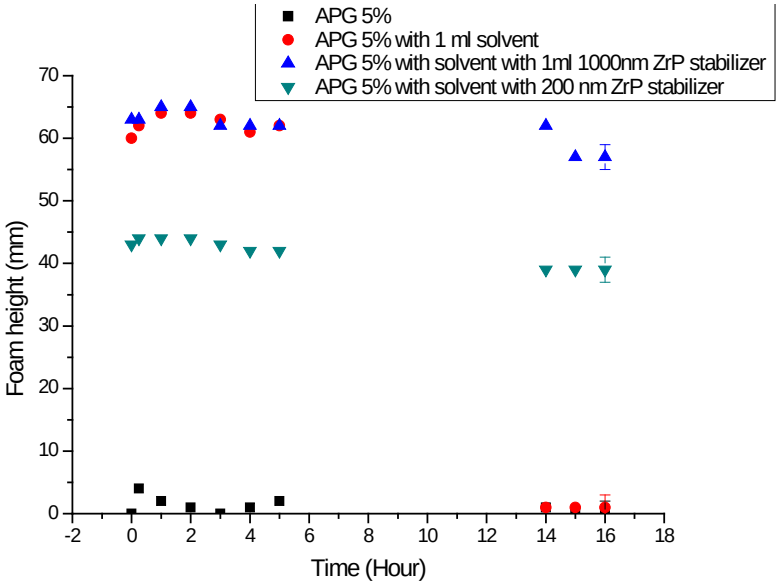

Figure 13. APG based different formulas volume change with time

SDS based high expansion foam formula

However, the APG formula is only an AFFF formula, which cannot accurately represent stability of high expansion foam by adding ZrP stabilizer. An ionic surfactant SDS based high expansion foam was adopted from US PATENT 444201851[56], which was

annotated as Hi-Ex#2 and applied in the experiment. The Hi-Ex#2 formula is composited by Poly Acrylic Acid (PAA), Butanol, Sodium dodecyl sulfate (SDS) and Decanol. The foam concentrate ingredients of this formula are listed in Table 3. In practice, this foam concentrate will be diluted 10 folds.[56] Hence, in our experiment, a 20% of the foam concentrate was prepared and stock for mixing with equal volume of ZrP stabilizer or DI water, so that final concentration of foam liquid would be 10% of the original one. A test was carried out with 4 different foam formulas, including 1 ml 20% high expansion foam concentrate and 1 ml DI water as control, 1 ml 20% high expansion foam concentrate and 1ml 1 w.t. % 200nm ZrP-PA foam stabilizer, 1 ml 20% high expansion foam concentrate and 1ml 1 w.t. % 1000nm ZrP-PA foam stabilizer, 1 ml 20% high expansion foam concentrate and 1ml 2 w.t. % 200nm ZrP-PA foam stabilizer. Hi-Ex#2 shows the stabilities of formulas with ZrP additives had great improvements compared to the control group which with DI water only as shown in Figure 14. Moreover, for different particle size and concentrations, the ZrP concentrated formula was not as stable as the less concentrated ones, the smaller size one (low aspect ratio) is not as stable as the larger one (high aspect ratio), which were in consistent with all the result stated in Guevara's paper[21]. Because the foams are generated by shaking, even for a same formula different trials may produce different volumes. So when comparing the foam stability we can normalized the foam volume by dividing the initial volume for different formula, that helps identify the difference between different formulas (as shown in Figure 15). Also we want to mention, for foam stability evaluation a new image taking system was introduced in to my experiment for more accurate image taking.

Pictures were taken by a webcam connected to computer. A software called 'Timelapse.exe' was used for taking pictures at setting time automatically.

We fitted the data in Figure 15 for the drainage process part with exponential decaying function:

$$\mathrm{N(t)} = N_0 e^{-\frac{1}{\tau}t} + O \qquad \text{4-1}$$

Where τ is the mean life time of the foam, from fitted plotting we acquired mean life time for different foams (Table 4). The mean life time of ZrP-PA nanoplatelets stabilized foam is dramatically increased by 10 to 20 times.

Table 3 Foam concentrate formula for SDS based high expansion foam

Foam concentrate formula of SDS based high expansion foam	
PAA	2 w.t.%
Butanol	10 w.t.%
SDS	8 w.t.%
Decanol	2 w.t.%
DI Water	78 w.t.%

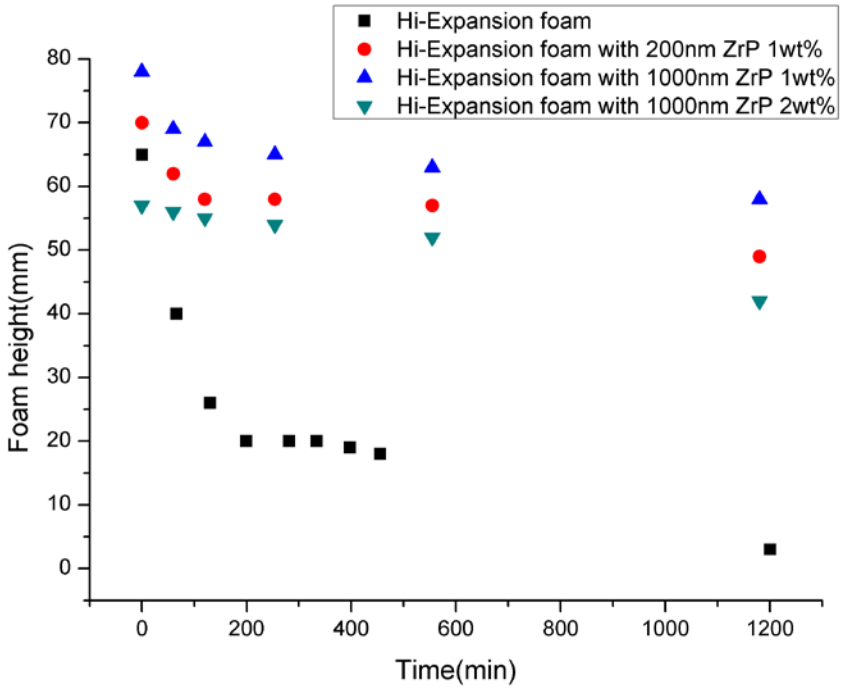

Figure 14. Hi-Ex #2 based different foam formulas volume change with time

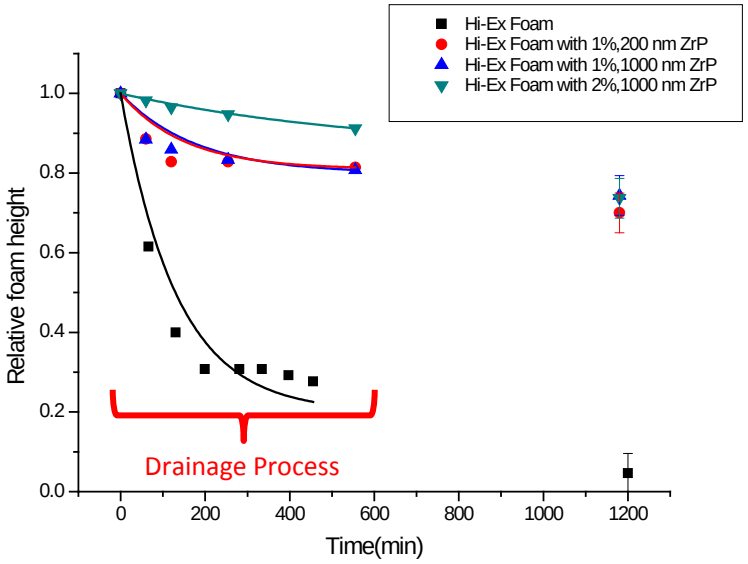

Figure 15. Normalized Hi-Ex #2 based different foam formulas volume change with time

Table 4 Mean life times for different foam formulas from data fitting

Foam formula	Mean life time
Hi-Ex Foam	221 ± 31 min
Hi-Ex Foam with 1%,200 nm ZrP	1934 ± 526 min
Hi-Ex Foam with 1%,1000 nm ZrP	1907 ± 599min
Hi-Ex Foam with 2%,1000 nm ZrP	5532 ± 500 min

Commercialized C2 high expansion foam formula

After ZrP stabilizer was tested with Hi-Ex #2 formula, we acquired some high expansion foam formula sample from Bin Zhang in Dr. Mannan's group. The formula has a commercialized name of 'Chemguard C2'. The foam volume stability test was also conducted. The formula with ZrP additive was stabilized well. However with several trials the expansion ratio of the ZrP added 'Chemguard C2' foam couldn't reach as high as the designed ratio. And even couldn't reach the expansion ratio of the control group. The reason could be the method we generate foam. These foams are designed to be applied by foam generator, not hand-shaken method. Also the ingredient of the C2 foam could react with ZrP platelets. From our knowledge ZrP can only exist in a narrow pH range. Either H+ or OH- can react with ZrP. The pH of the C2 foam is slightly basic. Some ingredient in the foam formula could be a potential reactor with the ZrP stabilizer. Optical micrographic pictures of the ZrP stabilized C2 foam and common C2 foam bubbles were taken with a Nikon TE-2000U microscope, the lense was setting to 30 X

magnification. Figure 16 Picture A shows the foam bubbles stabilized by C2 foam formula only. Picture B shows the foam bubbles stabilized by C2 foam formula and 2% weight percent1000nm ZrP-PA platelets. Picture C shows the foam bubbles stabilized by C2 foam formula and 2% weight percent 200nm ZrP-PA platelets. From the microscopic pictures we can tell the foam bubble without ZrP-PA platelets stabilizer is larger in size than the bubble with ZrP platelets. The sizes difference in bubble size is probably induced by the decreasing of interfacial tension in the ZrP stabilized system, in which the ZrP-PA platelet attaches on the liquid-gas interface. However, our particles size is around 200 to 1000nm scale and the exfoliated single layer of ZrP is single or several crystal layers. The ZrP-PA platelets are infeasible to be observed under optical microscope. The illumination intensity of the image system was kept same during the whole imaging process for these three different foam systems. Obviously in picture B and C the brightness is lower than picture A. The changing in brightness as a result of lower light transmittance of ZrP platelets proves the existence of ZrP-PA platelets in the foam system.

Other questions about foam morphology might be raised for the circular shape of the bubbles. According to previous research on foam morphology, high expansion foam should be dry foam whose shape should be polygon in general.[9] The circular shaped was caused by testing conditions in the microscope. Foam bubbles have to be taken out from original test tube and drooped on glass slide. This sample acquiring method ripped fragile dry foam and caused bubble coarsening. The excessive liquid from coarsening bubbles changed the gas-liquid ratio in the foam system and for that reason the foam

changed from dry foam to wet foam. We can see before sample acquiring, the foam system in test tube is polydron shaped dry foam, especially for the top part, as shown in Figure 17.

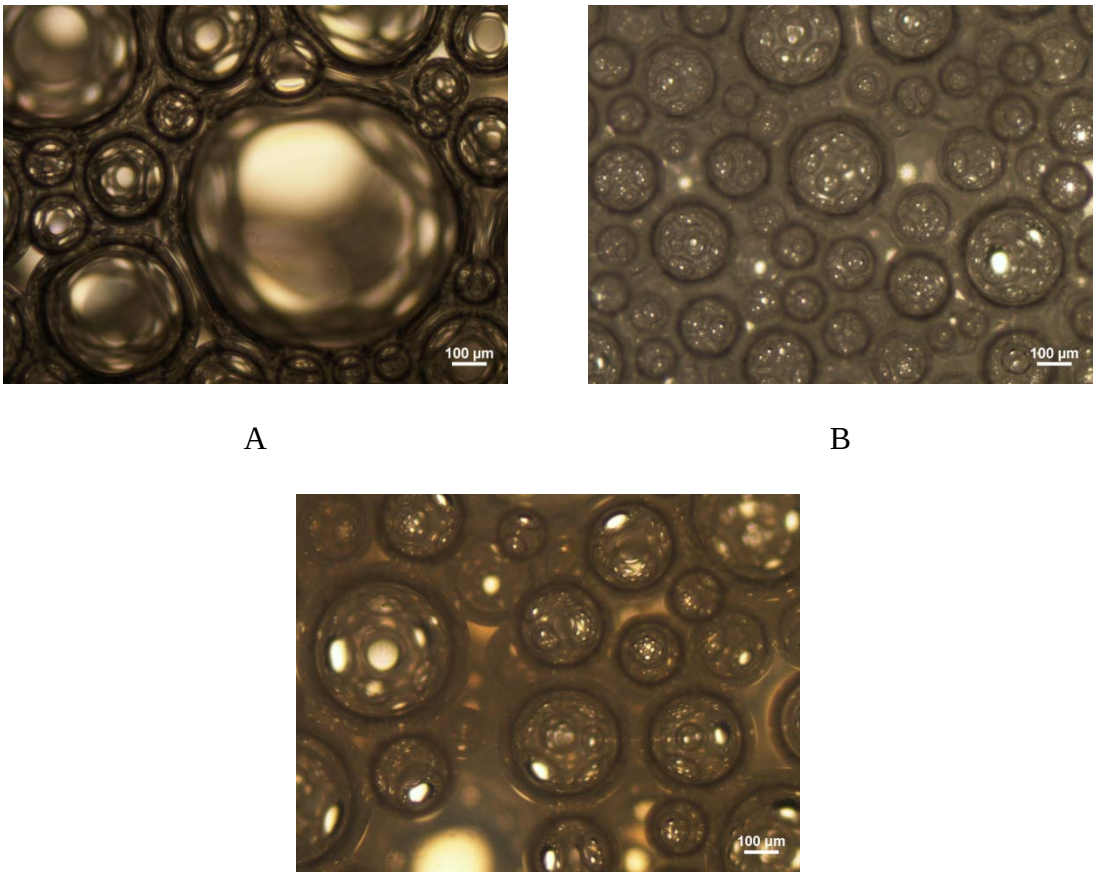

A B

C

Figure 16. Picture A shows the foam bubbles stabilized by C2 foam formula only. Picture B shows the foam bubbles stabilized by C2 foam formula and 2% weight percent1000nm ZrP-PA platelets. Picture C shows the foam bubbles stabilized by C2 foam formula and 2% weight percent 200nm ZrP-PA platelets.

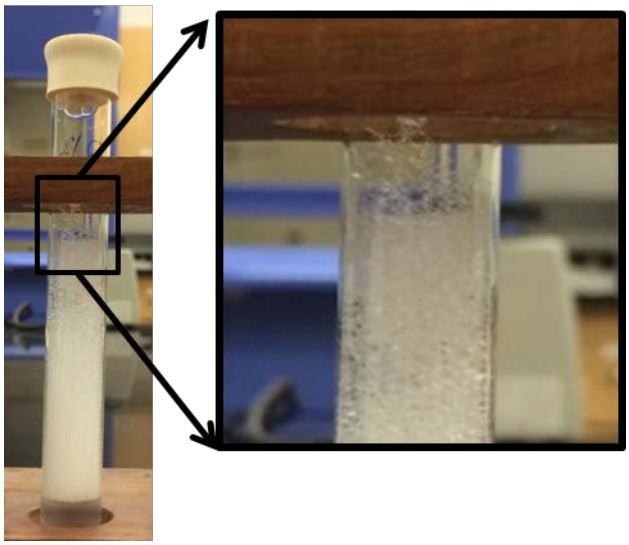

Figure 17. 2% C2 foam in tube shows the dry foam produced in test tube

Foam stability test under extreme conditions

The other advantage of the Janus platelet surfactant is that local concentration of the effective surfactant won't be affected by temperature or salinity in the system too much. Since we use the Janus platelets to stabilize the foam structure, the foam should be also more stable under high salinity condition. In this trial, we added 0.5% NaCl solution into the test tube and mixed with APG-2 formula. The reason to choose APG-2 formula is APG is more susceptible with salinity change. The formula with 2% 200nm ZrP-PA is more stable than the control group (Figure 18). The normalized result can provide further evident for the exceptional stability of the formula with ZrP-PA compared to the control group (Figure 19). The drainage section of normalized foam stability is also fitted with exponential decaying model. The mean life time for high expansion foam formula is 93$\pm$12 minutes and mean life time for high expansion foam formula with 2 w.t. % 200nm ZrP is 427$\pm$62 minutes. Compared to the foams with DI water, both foam

formulas experienced a stability decaying. However, the foam with ZrP-PA stabilizer is still more stable than the normal foam.

The other interesting observation is the form ripening induced volume change is postponed in the experiment with ZrP stabilizer (Shown as Figure 19). As reported in previous papers[21, 57], high stability is an special advantage for solid particle stabilized foam and the high stability can be attributed to platelets reducing the ripening process[9]. The redistribution of gas in the bubble will be greatly hindered by the platelets between bubbles, especially when the gas permeability of platelets is low. Application by using ZrP nanocomposite as a gas barrier is also mentioned in literature[42].

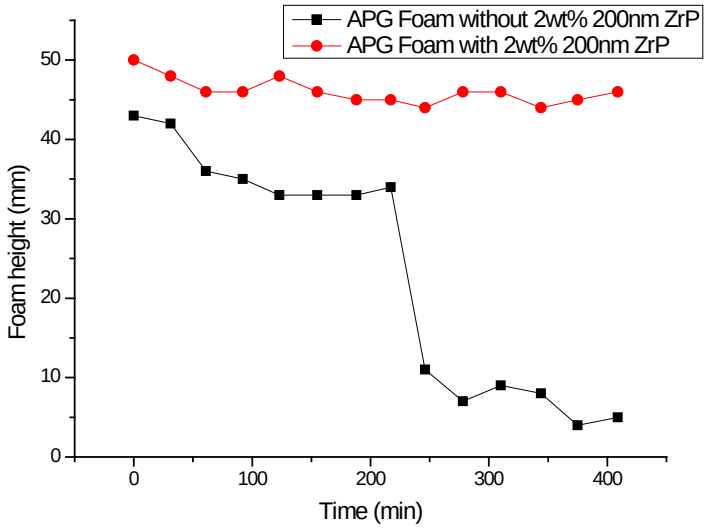

Figure 18. Foam volume change with 0.5% NaCl solution (APG formula)

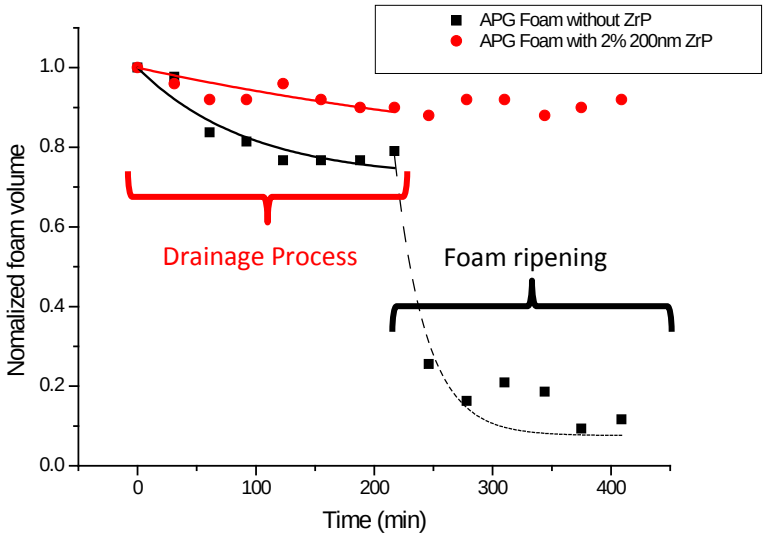

Figure 19. Normalized foam volume change with 0.5% NaCl solution (APG formula)

Also we measured the stability of ZrP-PA stabilized foam under low temperature condition. In the experiment, two samples are immersed into ice-water mixture (Figure 20), so that the temperature can be maintained around 0 ℃ . One with ZrP-PA stabilizer with Hi-Ex #2 formula and another is control group with Hi-Ex #2 formula only.

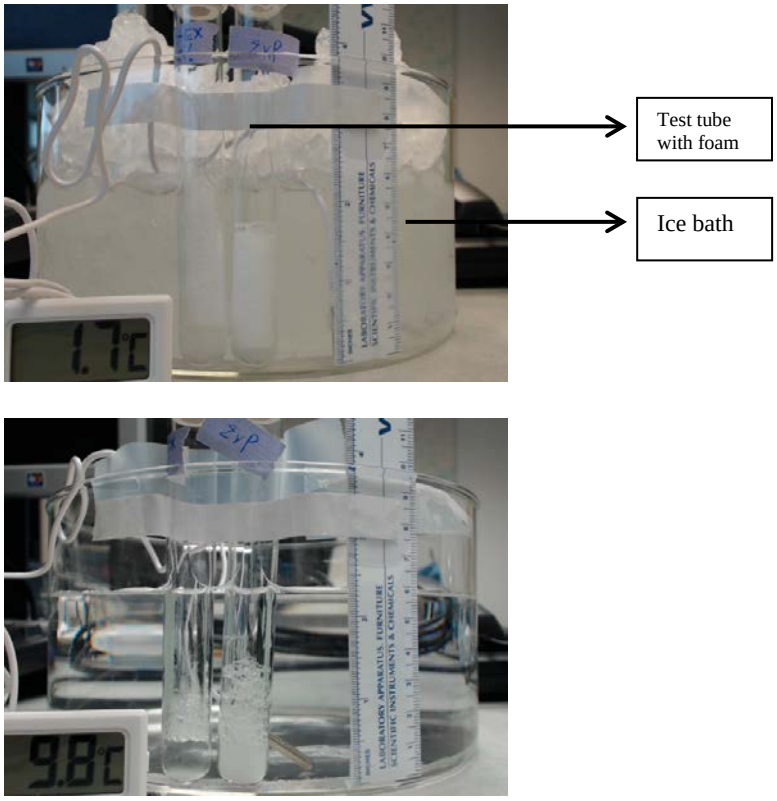

Figure 20. Ice bath test (Left) Initial picture of foam stabilized by ZrP-PA and foam without ZrP-PA. (Right), pictures after testing.

Figure 21 shows the foam volume change with time for samples stabilized by ZrP-PA and without ZrP-PA. The initial foam volume difference is due to the foam generation method. Foam generated by hand-shake method cannot always ensure the uniformity of the foam volume and the expansion ratio is not comparable with the foam expansion ratio generated by foam generator. So in Figure 22 we normalized the foam volume by dividing the foam volume with initial foam volume, which presents a better trend comparing for both experiment objects. Also, the drainage section of normalized foam stability is fitted with exponential decaying model. The mean life time for high expansion foam formula is 194±16 minutes and mean life time for high expansion foam

formula with 2 w.t. % 200nm ZrP is 1589±338 minutes. Compared to the foams in room temperature both foam formulas experienced a stability decaying. However, the foam with ZrP-PA stabilizer is still more stable than the normal foam.

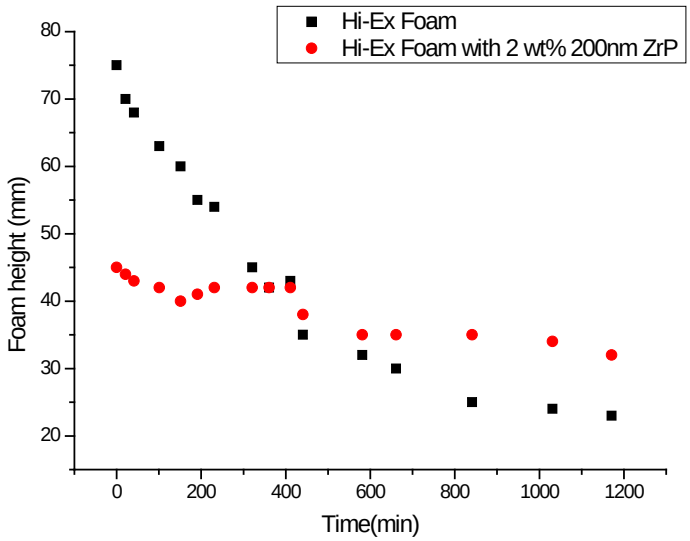

Figure 21. Foam stability under 0 ℃

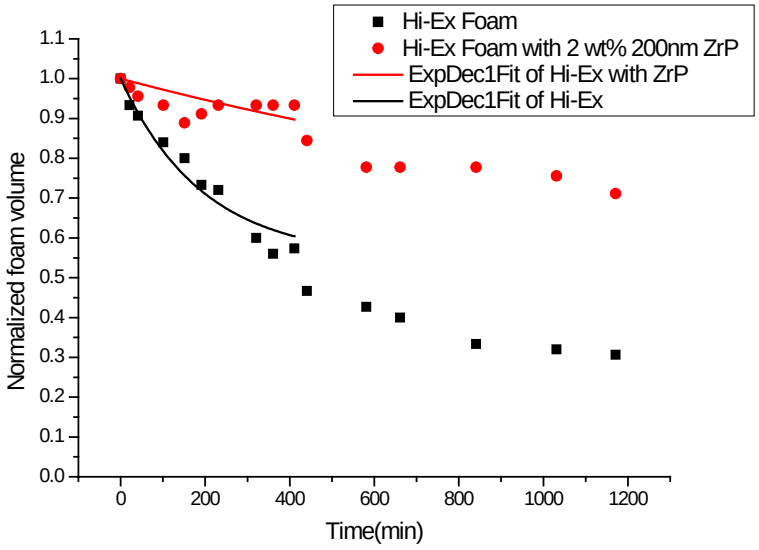

Figure 22. Normalized foam stability under 0 ℃

Foam drainage test

The increased stability for the foam volume can be understood as the behavior of ZrP platelets on the gas-liquid interface as we stated in formula 1-6, which is

$$E = \pi r^2 \gamma_{interface}(1 \pm \cos\theta)^2$$

In this formula the disk size and interfacial tension are taken in to consideration. The stability of the platelets on the surface is related with the particle diameter, interfacial tension and contact angle. However, this formula only describes the stability of the platelets on the boundary which related with the foam ripening.

A comprehensive mechanism for the ZrP-PA foam stabilization will be appreciated if the foam drainage can be accounted. Drainage is the procedure describing liquid losing from the foam part. In our experiment we generated foam with different formulas and drop a dye on to the foam. The dye will diffuse into the aqueous part of the foam

and flow with the liquid within the channel between foam bubbles. The propagation speed of the dye can be treated as the drainage flow rate. By acquiring image at different time, we can calculate out the drainage flow rate for the liquid drainage in the foam. In the experiment we use the methyl blue to dye the water phase and show propagation speed of water drainage. Figure 23 shows the drainage rate for the foam based on Hi-Ex #2 formula with 2 w.t.% ZrP-PA and without ZrP-PA. The drainage rate shows the ZrP-PA particles hindered water drainage rate by about 66% (Figure 23). The low drainage rate is resulted from the hydrophobic surface modification of the ZrP platelets.

As shown in Figure 24, in the molecular surfactant model the drainage flow will disturb surfactant molecules on the interface. The fluctuation resulted from drainage flow sometimes can induce local surfactant concentration dilution or micelles formation, which rarely considered by peer researchers. On the contrast, in our ZrP-PA nano platelets surfactant system, the surfactant would attach on the air-liquid surface firmly. It needs more energy input for flow drainage or Brownian emotion to shuffle the surfactant on the interface. Hence, the surface tension would be more stable compared to the molecular surfactant.

However, different from the thermal fluctuation, the reducing in drainage rate is mainly because the hydrophobic modification in the nano platelets surfactant system. The hydrophobic branches pointing towards the water channel modify the drainage channel slightly hydrophobic, shown as Figure 25. The hydrophobic channel hindered the drainage induced by gravity. So, this information provides us further possibilities to

modify the surface with more hydrophobic material to further reduce the drainage rate and stabilize foam.

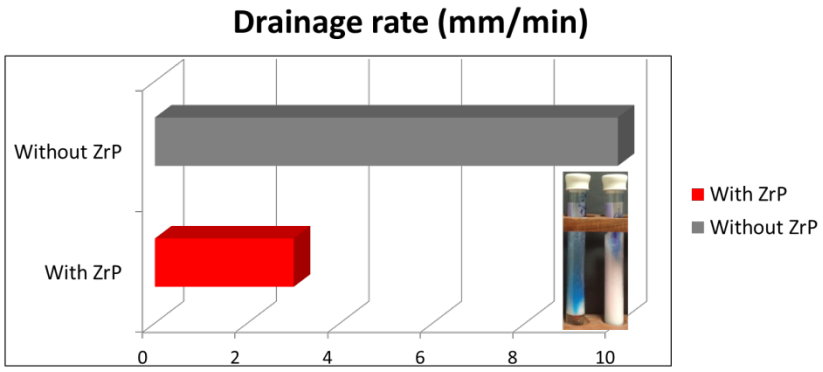

Figure 23. Drainage rate measured by dye moving rate in mm per minute (Hi-Ex #2 formula)

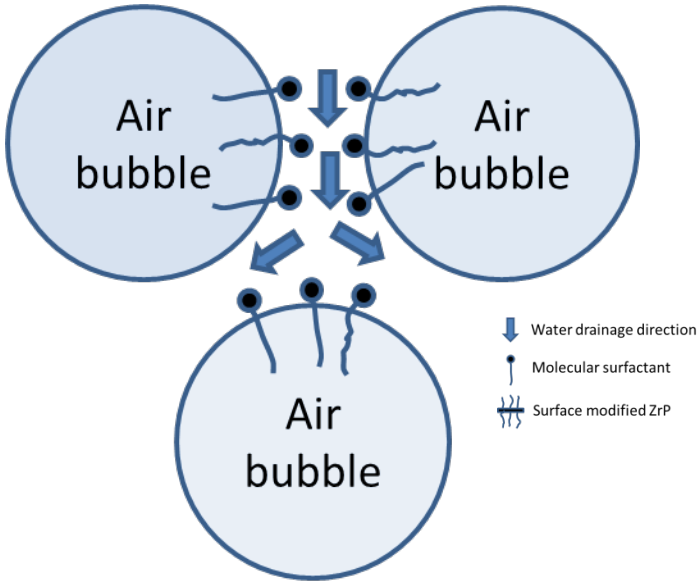

Figure 24. Water drainage in foam when only with molecular surfactant

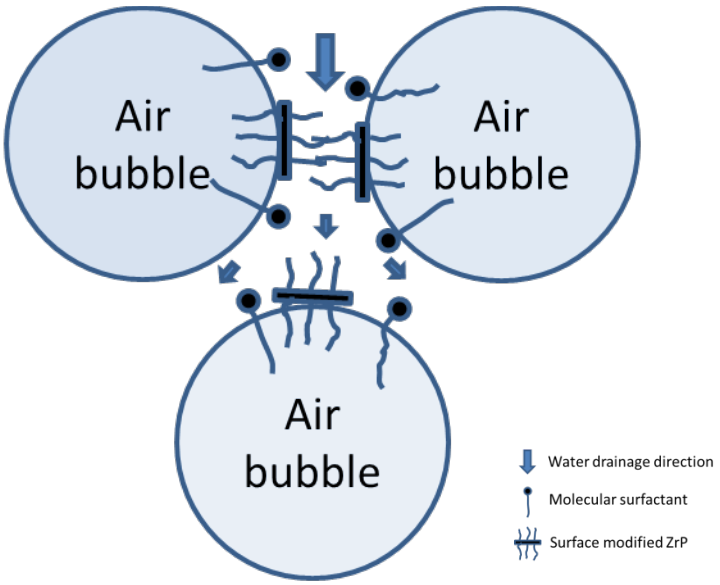

Figure 25. Water drainage in foam with molecular surfactant and ZrP Stabilizer (Reduced drainage rate)

LN_2 simulated vaporization test

The function of high expansion foam applied on the spilled LNG has been studied in detail by peer researchers.[20, 49] Researches show high expansion foam mainly has blanket effect and buoyancy increasing effect on the evaporated LNG. To measure the effectiveness of different high expansion foams, a quantitative method should be developed. As the experiment conducted in Bin's paper,[49] LN_2 is a good model to simulate vaporization of LNG. By measuring the mass of LN_2 covered by foam and fitting mass change with time we can get the evaporating speed of LN_2 covered by foam. The experiment set up is designed as Figure 26 shows. A balance with accuracy of 0.0005kg was used to measure the mass change by the evaporation of LN_2 and a computer was used to record the changing mass number on the balance by taking

pictures 10 seconds a frame. Different LN_2 containers were tried for better insulation. Firstly, a 500 ml beaker (shown as Figure 26) was employed to contain LN_2 during the test. To further reduce the heat conduction from side and bottom several insulation sponge and aluminum foil were used. About 200 ml LN_2 was poured into the container, then waiting for 5-10 minutes to let the system reach thermal equilibrium. Part of the LN_2 would vaporize during this time. After this 20 ml 10% Hi-Ex #2 foam and 2% ZrP-PA mixture would be shaken in test tube to generate foam and poured on the LN_2 surface. Foam would solidified on the freezing LN_2 surface (-196℃) several second after contact LN_2. A camera from the laptop computer kept recording the weight numbers shown on the screen of electronic balance.

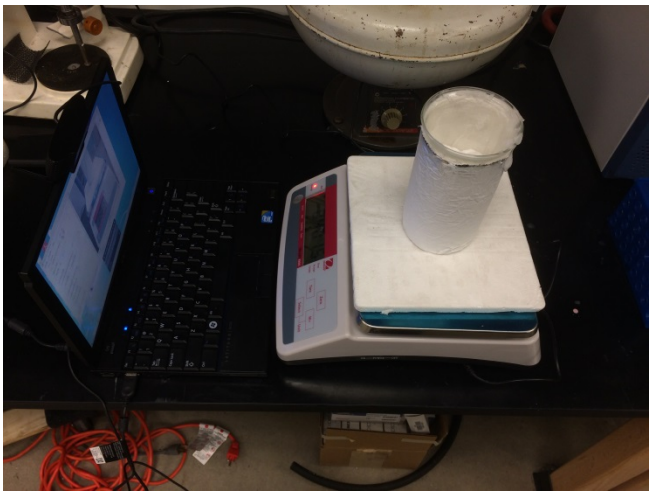

Figure 26. The set up to measure LN_2 vaporization speed

Figure 27 shows the frozen foam in the beaker, which is equivalent with the view through insulation layer covered beaker. From the picture, we observed about 100ml

foam were generated and covered on the LN_2 surface. It showed the low efficiency of the hand-shaking foam generation.

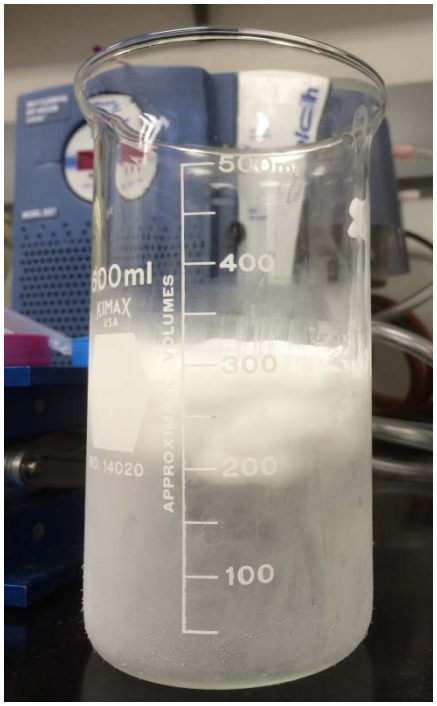

Figure 27. Vertical view of the frozen foam

To measure the vaporization rate of LN_2, different formulas and a blank control group were tried separately. By linear fitting the mass with time, we can get the slope of the mass changing function and the slope represents the vaporization rate of the LN_2 (Figure 28). From the fitting result we can see the vaporization speed for LN_2 covered by ZrP-PA mixed Hi-Ex #2 foam is $(-4.96 \pm 0.08) \times 10^{-5}$ kg/s, which is 9% slower than the pure Hi-Ex #2 foam. This is probably because of ZrP's low heat conductivity 0.199 $W/(m \times K)$ (@−162 ℃), compared to ice about 1 $W/(m \times K)$ under same temperature. However, by compared between the blank control and the one with Hi-Ex

#2 covered group, we found the vaporization speed is almost the same, which means the heat conduction from side wall and bottom of the beaker was still dominating the vaporization process and the system didn't reach thermal equilibrium state. A better container design needs to be called.

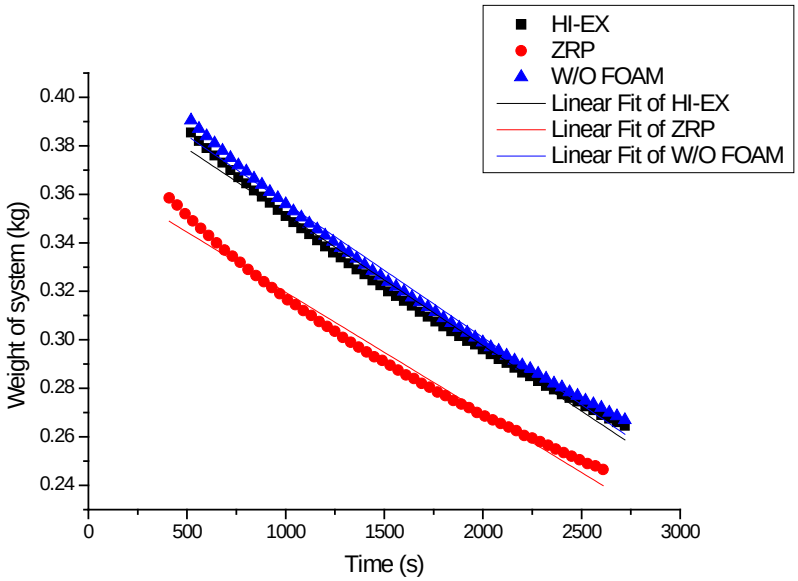

Figure 28. Weight change of the Beaker system

Table 5 Data fitting result for the beaker container

	Slope (vaporization rate)	Standard Error	R-Square
Without covering	-5.54× 10^{-5}	0.06 × 10^{-5}	0.9927
With Hi-Ex foam covering	-5.41× 10^{-5}	0.06 × 10^{-5}	0.9922
With ZrP stabilized Hi-Ex foam covering	-4.96× 10^{-5}	0.08 × 10^{-5}	0.9859

A cryogenic container was purchased from Chemglass Company. This container is a layered design with vacuum between two glass layers. Still 3 different group were taking separately. In first group, about 200 ml LN_2 was poured into the container and left for evaporation without any foam covered. In second group, about 200 ml LN_2 was poured into the container, then waiting for 5-10 minutes to let the system reach thermal equilibrium. After this 20 ml 10% Hi-Ex #2 foam and 2% ZrP-PA mixture would be shaken in test tube to generate foam and poured on the LN_2 surface. In the third group pure Hi-Ex #2 foam was used without ZrP-PA surfactant. The mass changing and vaporization rate fitting are shown in Figure 29. The fitting result in Table 5 shows with the better insulated container, the system can reach thermal equilibrium now. Compared to the uncovered LN_2 system, evaporation rate in both ZrP-PA system and Hi-Ex #2 systems were reduced by about 25%. However, compared between ZrP-PA and Hi-Ex #2 system evaporating speed is only reduced by 5% (Table 6). Foam with ZrP-PA doesn't show much improvement compared to conventional foam. One of the reason is because the foam isn't thick enough to differentiate blanket effect between two foam formulas.

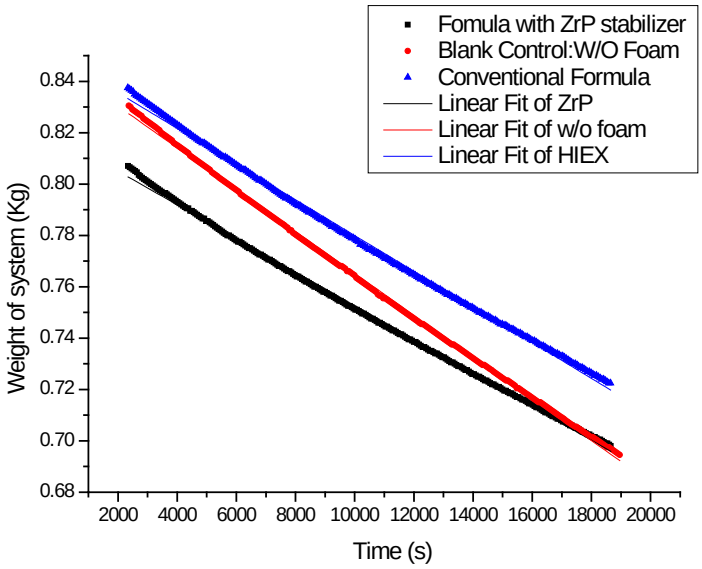

Figure 29. Weight change of the cryogenic system

Table 6 Data fitting result for the cryogenic container

	Slope (vaporization rate)	Standard Error	R-Square
Without covering	-8.14× 10^{-6}	0.01 × 10^{-6}	0.9991
With Hi-Ex foam covering	-6.95× 10^{-6}	0.02 × 10^{-6}	0.9979
With ZrP stabilized Hi-Ex foam covering	-6.54× 10^{-6}	0.02 × 10^{-6}	0.9982

CHAPTER V

CONCLUSION

Enlightened by Pickering emulsion of oil-water phases mixture, ZrP-PA nanoplatelets are first time used as a surfactant to stabilized high expansion foams. Three different types of firefighting foams and LNG suppression foam were used as models to investigate foam properties stabilized by ZrP nanoplatelets. The research results showed foam stability was improved by adding ZrP-PA stabilizer into high expansion foam and firefighting foam formulas. The foam stability is improved by 70% by measuring foam volume change with time in group with 2% 200nm ZrP-PA addition. Further experiments show the ZrP-PA stabilized foam has a better stability under extreme conditions, including high salinity and low temperature. To investigate the mechanism of foam stabilization with nanoplatelets, a drainage rate experiment was carried out. Results showed that high expansion foams with ZrP-PA shows a slower drainage rate, which is 30% of the common high expansion foam. Combined with the low gas permeability induced ripening delaying and the thermodynamic analysis of platelets adsorption on the gas-liquid interface, it can well explain the reason why foams with ZrP-PA nanoplatelets were more stable than normal foam. Also, a liquid nitrogen gas evaporation experiment was conducted to simulate the evaporation of LNG. A modest decrease in evaporation rate is observed due to the foam volume applied on LNG.

To further develop this technique in the near future, more foam formulas should be tested with the different platelets system and different surface modification. An

automatic foam generator should be constructed to eliminate variance from the foam generating procedures.

REFERENCES

1. Hiltz, R. H.; Greer, J. S.; Friel, J. V., Fire-fighting foam. US Patent 4,713,182.1987.

2. Farajzadeh, R.; Andrianov, A.; Krastev, R.; Hirasaki, G. J.; Rossen, W. R., Foam-oil interaction in porous media: Implications for foam assisted enhanced oil recovery. *Adv Colloid Interfac* **2012,** *183*, 1-13.

3. Arzhavitina, A.; Steckel, H., Foams for pharmaceutical and cosmetic application. *Int J Pharmaceut* **2010,** *394*, 1-17.

4. Poole, B. Ordinary people and effective operation of fire extinguishers. Eastern Kentucky University, Richmond, KY 2012, http://www.femalifesafety.org/docs/wpistudyfinal.pdf.

5. Alm, R. R.; Stern, R. M., Aqueous film-forming foamable solution useful as fire extinguishing concentrate. US Patent 5,085,786.1992.

6. Boyd, C. F.; Di Marzo, M. Fire protection foam behavior in a radiative environment. research directed by Dept. of Mechanical Engineering.University of Maryland at College Park 1996, http://fire.nist.gov/bfrlpubs/fire96/PDF/f96079.pdf.

7. Lattimer, B. Y.; Trelles, J., Foam spread over a liquid pool. *Fire Safety Journal* **2007,** *42*, 249-264.

8. Gardiner, B.; Dlugogorski, B.; Jameson, G., Rheology of fire-fighting foams. *Fire Safety Journal* **1998,** *31*, 61-75.

9. Stevenson, P., *Foam engineering: fundamentals and applications*. John Wiley & Sons, New York2012.

10. Joseph, D. D., Questions in fluid mechanics: Understanding foams and foaming. *Journal of Fluids Engineering* **1997,** *119*, 497-498.

11. Tempel, M.; Lucassen, J.; Lucassen-Reynders E. H., Application of surface thermodynamics to Gibbs elasticity. *J Phys Chem-Us* **1965,** *69*, 1798.

12. Binks, B. P., Particles as surfactants—similarities and differences. *Current Opinion in Colloid & Interface Science* **2002,** *7*, 21-41.

13. Binks, B. P.; Lumsdon, S. O., Catastrophic phase inversion of water-in-oil emulsions stabilized by hydrophobic silica. *Langmuir* **2000,** *16*, 2539-2547.

14. Binks, B. P., Particles as surfactants - similarities and differences. *Current Opinion in Colloid & Interface Science* **2002,** *7*, 21-41.

15. U.S. Energy Information Administration (EIA), International Energy Statistics. Date retrieved from online chart (http://www.eia.gov/totalenergy/data/annual/) **2013**.

16. Głomski, P.; Michalski, R., Problems with determination of evaporation rate and properties of boil-off gas on board LNG carriers. *Journal of Polish CIMAC* **2011,** *6*, 133-140.

17. Alderman, J. A., Introduction to LNG safety. *Process Saf Prog* **2005,** *24*, 144-151.

18. Foss, M. M.; Delano, F.; Gulen, G.; Makaryan, R., LNG safety and security. *Center for Energy Economics (CEE)* **2003**.

19. Hightower, M.; Gritzo, L.; Luketa-Hanlin, A.; Covan, J.; Tieszen, S.; Wellman, G.; Irwin, M.; Kaneshige, M.; Melof, B.; Morrow, C. *Guidance on risk analysis and safety implications of a large liquefied natural gas (LNG) spill over water*; DTIC Document2004.

20. Takeno, K.; Ichinose, T.; Tokuda, K.; Ohba, R.; Yoshida, K.; Ogura, K., Effects of high expansion foam dispersed onto leaked LNG on the atmospheric diffusion of vaporized gas. *J Loss Prevent Proc* **1996,** *9*, 125-133.

21. Guevara, J. S.; Mejia, A. F.; Shuai, M.; Chang, Y.-W.; Mannan, M. S.; Cheng, Z., Stabilization of Pickering foams by high-aspect-ratio nano-sheets. *Soft Matter* **2013,** *9*, 1327-1327.

22. Liu, Q.; Luan, L.; Sun, D.; Xu, J., Aqueous foam stabilized by plate-like particles in the presence of sodium butyrate. *J. Colloid Interface Sci.* **2010,** *343*, 87-93.

23. Liu, Q.; Zhang, S.; Sun, D.; Xu, J., Foams stabilized by Laponite nanoparticles and alkylammonium bromides with different alkyl chain lengths. *Colloids and Surfaces A: Physicochemical and Engineering Aspects* **2010,** *355*, 151-157.

24. Tang, F.-Q.; Xiao, Z.; Tang, J.-A.; Jiang, L., The effect of SiO< sub> 2</sub> particles upon stabilization of foam. *J. Colloid Interface Sci.* **1989,** *131*, 498-502.

25. Horozov, T. S.; Binks, B. P., Particle‐Stabilized emulsions: A bilayer or a bridging monolayer? *Angewandte Chemie* **2006,** *118*, 787-790.

26. Vilkova, N. G.; Elaneva, S. I.; Karakashev, S. I., Effect of hexylamine concentration on the properties of foams and foam films stabilized by Ludox. *Mendeleev Commun* **2012,** *22*, 227-228.

27. Kruglyakov, P. M.; Elaneva, S. I.; Vilkova, N. G., About mechanism of foam stabilization by solid particles. *Adv Colloid Interfac* **2011,** *165*, 108-116.

28. Johansson, G.; Pugh, R., The influence of particle size and hydrophobicity on the stability of mineralized froths. *Int J Miner Process* **1992,** *34*, 1-21.

29. Dippenaar, A., The destabilization of froth by solids. II. The rate-determining step. *Int J Miner Process* **1982,** *9*, 15-22.

30. Fameau, A. L.; Saint‐Jalmes, A.; Cousin, F.; Houinsou Houssou, B.; Novales, B.; Navailles, L.; Nallet, F.; Gaillard, C.; Boué, F.; Douliez, J. P., Smart foams: switching reversibly between ultrastable and unstable foams. *Angewandte Chemie International Edition* **2011,** *50*, 8264-8269.

31. Madivala, B.; Vandebril, S.; Fransaer, J.; Vermant, J., Exploiting particle shape in solid stabilized emulsions. *Soft Matter* **2009,** *5*, 1717-1727.

32. Vijayaraghavan, K.; Nikolov, A.; Wasan, D., Foam formation and mitigation in a three-phase gas–liquid–particulate system. *Adv Colloid Interfac* **2006,** *123*, 49-61.

33. Gonzenbach, U. T.; Studart, A. R.; Tervoort, E.; Gauckler, L. J., Tailoring the microstructure of particle-stabilized wet foams. *Langmuir* **2007,** *23*, 1025-1032.

34. Vilkova, N. G.; Elaneva, S. I.; Kruglyakov, P. M.; Karakashev, S. I., Foam films from hexylamine stabilized by the silica particles. *Mendeleev Commun* **2011,** *21*, 344-345.

35. Tran, D. N.; Whitby, C. P.; Fornasiero, D.; Ralston, J., Foamability of aqueous suspensions of fine graphite and quartz particles with a triblock copolymer. *J. Colloid Interface Sci.* **2010,** *348*, 460-468.

36. Hudales, J.; Stein, H., The influence of solid particles on foam and film drainage. *J. Colloid Interface Sci.* **1990,** *140*, 307-313.

37. Clearfield.A; Smith, G. D., Crystallography and structure of Alpha-Zirconium bis(monohydrogen orthophosphate) monohydrate. *Inorg Chem* **1969,** *8*, 431.

38. Clearfield, A.; Stynes, J. A., The preparation of crystalline zirconium phosphate and some observations on its ion exchange behaviour. *J Inorg Nucl Chem* **1964,** *26*, 117-129.

39. Clearfield, A., Hydrothermal synthesis of selected phosphates and molybdates. *Prog Cryst Growth Ch* **1991,** *21*, 1-28.

40. Mejia, A. F.; Diaz, A.; Pullela, S.; Chang, Y.-W.; Simonetty, M.; Carpenter, C.; Batteas, J. D.; Mannan, M. S.; Clearfield, A.; Cheng, Z., Pickering emulsions stabilized by amphiphilic nano-sheets. *Soft Matter* **2012,** *8*, 10245-10245.

41. Clearfield, A.; Ortizavila, C. Y., Polyether and polyimine derivatives of layered zirconium-phosphates as supramolecules. *Supramolecular Architecture* **1992,** *499*, 178-193.

42. Sun, L. Y.; Boo, W. J.; Sun, D. H.; Clearfield, A.; Sue, H. J., Preparation of exfoliated epoxy/alpha-zirconium phosphate nanocomposites containing high aspect ratio nanoplatelets. *Chemistry of Materials* **2007,** *19*, 1749-1754.

43. Ortizavila, C. Y.; Clearfield, A., Polyether derivatives of zirconium-phosphate. *Inorg Chem* **1985,** *24*, 1773-1778.

44. Yamanaka, S., Synthesis and characterization of the organic derivatives of zirconium phosphate. *Inorg Chem* **1976,** *15*, 2811-2817.

45. Nakamura, K.; Matsuyama, K.; Tomita, I.; Hasegawa, Y., Intercalation of n-alkylamines and n-alkyldiamines into gamma-zirconium phenylphosphonate phosphate. *J Inclus Phenom Mol* **1998,** *31*, 351-355.

46. MacLachlan, D. J.; Morgan, K. R., Phosphorus-31 solid-state NMR studies of the structure of amine-intercalated. alpha.-zirconium phosphate. 2. Titration of. alpha.-zirconium phosphate with n-propylamine and n-butylamine. *The Journal of Physical Chemistry* **1992,** *96*, 3458-3464.

47. Alberti, G.; Casciola, M.; Costantino, U., Inorganic ion-exchange pellicles obtained by delamination of alpha-zirconium phosphate crystals. *J. Colloid Interface Sci.* **1985,** *107*, 256-263.

48. Clearfield, A.; Tindwa, R. M., On the mechanism of ion exchange in zirconium phosphates—XXI Intercalation of amines by α-zirconium phosphate. *Journal of Inorganic and Nuclear Chemistry* **1979,** *41*, 871-878.

49. Zhang, B.; Liu, Y.; Olewski, T.; Vechot, L.; Mannan, M. S., Blanketing effect of expansion foam on liquefied natural gas (LNG) spillage pool. *J Hazard Mater* **2014,** *280*, 380-388.

50. Guevara, J. S.; Mejia, A. F.; Shuai, M.; Chang, Y. W.; Mannan, M. S.; Cheng, Z. D., Stabilization of Pickering foams by high-aspect-ratio nano-sheets. *Soft Matter* **2013,** *9*, 1327-1336.

51. Koehler, S. A.; Hilgenfeldt, S.; Stone, H. A., A generalized view of foam drainage: experiment and theory. *Langmuir* **2000,** *16*, 6327-6341.

52. Shuai, M.; Mejia, A. F.; Chang, Y.-W.; Cheng, Z., Hydrothermal synthesis of layered α-zirconium phosphate disks: control of aspect ratio and polydispersity for nano-architecture. *Crystengcomm* **2013,** *15*, 1970-1970.

53. Sun, L.; Boo, W. J.; Sue, H.-J.; Clearfield, A., Preparation of α-zirconium phosphate nanoplatelets with wide variations in aspect ratios. *New J Chem* **2007,** *31*, 39-43.

54. Chang, Y.-W.; Mejia, A. F.; Cheng, Z.; Di, X.; McKenna, G. B., Gelation via ion exchange in discotic suspensions. *Phys Rev Lett* **2012,** *108*, 247802.

55. Norman, E. C.; Regina, A. C., Alcohol resistant aqueous film forming firefighting foam. US Patent 5,207,932,1993.

56. Rand, P. B., Stabilized aqueous foam systems and concentrate and method for making them. US Patent 4,442,018, 1984.

57. Gonzenbach, U. T.; Studart, A. R.; Tervoort, E.; Gauckler, L. J., Ultrastable particle-stabilized foams. *Angewandte Chemie International Edition* **2006,** *45*, 3526-3530.